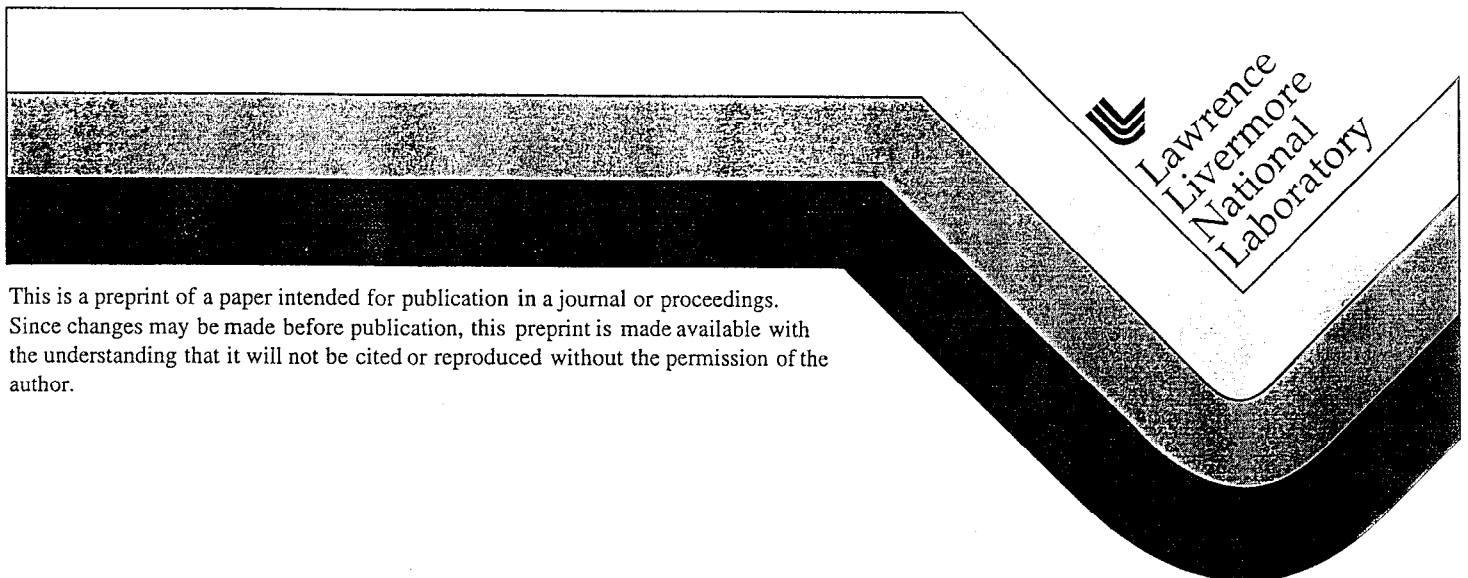


Multiscale Modeling of Radiation Effects in Fcc and Bcc Metals

T. Diaz de la Rubia
M. Caturla
E. Alonso
B. Wirth
M. Wall
T. Felter
M. Fluss
J. Perlado

This paper was prepared for submittal to the
International Conference on Mathematics and Computations 99
Madrid, Spain
September 26-29, 1999

July 15, 1999



This is a preprint of a paper intended for publication in a journal or proceedings.
Since changes may be made before publication, this preprint is made available with
the understanding that it will not be cited or reproduced without the permission of the
author.

DISCLAIMER

This document was prepared as an account of work sponsored by an agency of the United States Government. Neither the United States Government nor the University of California nor any of their employees, makes any warranty, express or implied, or assumes any legal liability or responsibility for the accuracy, completeness, or usefulness of any information, apparatus, product, or process disclosed, or represents that its use would not infringe privately owned rights. Reference herein to any specific commercial product, process, or service by trade name, trademark, manufacturer, or otherwise, does not necessarily constitute or imply its endorsement, recommendation, or favoring by the United States Government or the University of California. The views and opinions of authors expressed herein do not necessarily state or reflect those of the United States Government or the University of California, and shall not be used for advertising or product endorsement purposes.

MULTISCALE MODELING OF RADIATION EFFECTS IN FCC AND BCC METALS

T. Diaz de la Rubia, M.J. Caturla, E. A. Alonso, B.D. Wirth, M.A. Wall, T.A. Felter,
M.J. Fluss,

Chemistry and Materials Science Directorate
Lawrence Livermore National Laboratory
Livermore, CA 94450, USA

And

J.M. Perlado
Instituto de Fusion Nuclear
Universidad Politecnica de Madrid
28006-Madrid, Spain

ABSTRACT

The prospect of using computer simulations to calculate radiation-induced defect production and its influence on microstructure evolution and mechanical property changes during prolonged irradiation of nuclear materials has been a beckoning, yet elusive goal for many years. However, the enormous progress achieved in computational physics for calculating reliable, yet tractable interatomic potentials, coupled with vast improvements in computational power have brought this hope to near reality. In order to develop modeling and simulation tools for predicting the irradiation response of nuclear structural materials, models must be implemented and tested across all relevant length and time scales. We discuss the development and implementation of a modeling methodology that consists of the linkage and hierarchical use of *ab initio* electronic structure calculations, molecular dynamics (MD) simulations, and kinetic Monte Carlo (KMC) simulations. This methodology can describe length and time scales from nanometers to hundreds of microns and from picoseconds to years, respectively. The ideas are demonstrated in two applications. First, we describe simulations that describe the irradiation and subsequent isochronal annealing of Pb, a low melting point fcc metal, and compare the results to experiments. Second, we show how these methods can be used to investigate damage production and freely migrating defect formation in irradiated V, the key component of candidate low activation alloys for fusion energy applications.

Introduction

Fusion conditions impose very strict requirements on structural materials and may necessitate the development of new ones with tailored properties that can withstand high neutron fluxes at elevated temperatures over reactor lifetimes. Moreover, a requirement for shallow burial of these structural materials at the end of life of the plant imposes major restrictions on the classes of materials that may be used. Thus, it is necessary to develop and test new material classes that can be employed under these conditions, a process that is both very expensive and time consuming. Availability of a predictive multiscale modeling methodology would enable rapid prototyping of materials and would therefore help develop new ones with properties tailored to the fusion environment at reduced cost and time.

In order to develop modeling and simulation tools for predicting the irradiation response of fusion structural materials, models must be implemented and tested across all relevant length and time scales. Figure 1 shows a commonly used pictorial description of the various scales involved in modeling radiation effects in materials. While collision cascades produce defects on a time scale of tens of picoseconds, diffusion occurs over much longer time scales, of the order of seconds. The ensuing microstructure and property changes can take place over even longer time scales.

At the shortest length and time scales, the study of radiation effects requires that the displacement cascades generated along the path of the recoil products be well understood. These cascades result in the initial distribution of excess defects in the crystal, the so-called primary damage state, and have been the subject of intense study for many years [1,2]. However, their small volume ($V \approx 4 \times 10^6 \text{ \AA}^3$) and short lifetime ($\approx 10^{-11} \text{ s}$) make their investigation by experimental means very difficult and only indirectly through e.g. transmission electron microscopy (TEM) observation can the primary state of damage be inferred [3]. Model potential molecular dynamics (MD), by virtue of its simplicity and the appropriateness of the length scale (e.g., a cube of $2 \times 10^8 \text{ \AA}^3$ contains 10^7 atoms) is an extremely powerful tool to obtain atomic-scale information and physical insight into the mechanisms of radiation-induced defect production. MD simulations have in fact been used extensively in the last ten years for the purpose of modeling defect production for recoils in the 100's of eV to 50 keV range [for recent reviews see e.g. [1,2, 4-7]. At present, more than 100 million atoms can be treated realistically for time scales of the order of tens of picoseconds on the most powerful massively parallel computers.

At temperatures where the defects produced by the cascade are mobile, diffusion gives rise to complex interactions over macroscopic time scales that must be modeled with methods other than MD. In order to predict and understand the long time scale evolution of the system, it is critical to know how many of the defects produced are able to escape their nascent cascade and migrate through the lattice to produce microstructure, composition, and property changes. Traditionally, reaction-diffusion equations have been used to model defect kinetics and microstructure evolution [9-14]. This rate theory approach assumes that the system is homogeneous and isotropic, and has proven quite powerful over the years. More recently, with the advent of powerful desktop

workstations, Kinetic Monte Carlo (KMC) simulations have come to be widely used for the purpose of modeling defect microstructure evolution under irradiation [15-21]. KMC has several advantages over traditional rate theory mainly given by the fact that the method retains the atomic nature of the diffusion process and can therefore treat difficult issues such inhomogeneities in time and space induced by the displacement cascades, anisotropic diffusion, the growth and dissolution of defect clusters of all possible sizes, one dimensional migration, stress effects, and non-homogeneous microstructures. The result of a KMC simulation is a solution of the diffusion problem that provides information on the spatial and temporal evolution of the defect microstructure, including the rate of impurity precipitation, the rate of sessile dislocation loop accumulation in the matrix, the rate of arrival of point defects and glissile dislocation loops at dislocations, the rate of nucleation and growth of voids, and many other microstructural evolution features.

In this paper, we describe our modeling methodology, which consists of the linkage and hierarchical use of *ab initio* electronic structure calculations, molecular dynamics (MD) simulations, kinetic Monte Carlo (KMC). This methodology can describe length and time scales from nanometers to hundreds of microns and from picoseconds to years, respectively. We present two examples of how this hierarchical approach can be used to model damage production and accumulation in metals.

The multiscale linkage approach that we will undertake can be summarized as follows:

- I. ***Ab initio* and Molecular Dynamics:** Under irradiation, defects are produced in localized displacement events over nanometer and picosecond length and time scales, respectively. This is the so-called primary damage state and represents the source term for all subsequent microstructure and property changes. This stage must be modeled with **molecular dynamics** (MD) methods, which use as input interatomic potentials derived from first principles *ab initio* electronic structure calculations. In addition, *ab initio* planewave codes with ultrasoft pseudopotentials are used on massively parallel computers to calculate point defect and small defect clusters energetics, kinetics and their interaction with impurities.
- II. **MD/KMC linkage:** The primary state of damage from displacement cascades obtained by MD is used as input to the KMC calculations in the form of a spatial distribution of point defects, impurities and defect clusters. In addition, the *ab initio* results establish the database of activation barriers used to compute probabilities for defect hopping in the KMC simulations.
- III. **KMC:** Diffusion of these defects, their accumulation in the lattice, and their interaction with the chemistry and the microstructure occur over length and time scales of microns and seconds and must be modeled with **kinetic Monte Carlo and rate theory** methods. The output of the linked MD/KMC simulation is then a macroscopic distribution of accumulated damage in a lattice for a given set of irradiation conditions of recoil spectrum, flux, fluence and substrate temperature. This microstructure includes the density and size distribution of voids, the density of interstitial and vacancy-type defect clusters and dislocation loops, and the

possible segregation profile of impurity atoms and distribution of second phase precipitates.

In the remainder of this manuscript we present two examples of the application of these methodology. The first example involves Pb, a high-Z low melting point fcc metal in which displacement cascade effects are maximized. We show how defect clustering in the cascades leads to significant deviations in annealing kinetics from what may be expected in other materials. Critical to the success of any modeling endeavor is the concomitant validation of the results by tailored experiments. We present a detailed account of recent work at LLNL that accomplishes this validation and show how the simulations do indeed provide an excellent means for describing the kinetics of these complex systems. Second, we discuss damage production and accumulation in Vanadium, a prototypical bcc metal that is the main element in proposed low activation alloys for fusion applications. We refer the reader to published articles for details regarding the various simulation methodologies.

II. Damage Production in Pb: Simulations and experimental validation.

In this work [22], we simulated the evolution of the defect microstructure resulting from irradiation of Pb with 180keV Er⁺ at liquid Nitrogen temperature followed by an isochronal anneal to 70 C. The results were validated by comparison with experiments. The simulations consisted of a coupled molecular dynamics (MD) and kinetic Monte Carlo (KMC) calculation that follows the production and migration of defects during irradiation and subsequent isochronal annealing. In the experiments, the ions were implanted at a temperature of -179° C and the ensuing damage was annealed by increasing the temperature in a stepwise fashion by 50°C every 5 minutes. In the simulations, the time-temperature evolution of the density of point defects and defect clusters is calculated by coupling MD and KMC simulations. The results were compared with experimental observations for the same irradiation and annealing conditions. The experiments consisted of a set of transmission electron microscope (TEM) micrographs taken at different times during the anneal. The micrographs show the presence of loops after irradiation, the increase in loop density with temperature, and the disappearance of all the loops at temperatures of ~ 70°C. As we shall below, the experimental results and the simulations were found to be in excellent agreement.

The primary stage of the damage produced by the energetic recoils was calculated using MD. For this particular simulations we had to reproduce the damage of 180keV Er ions on Pb. We used a binary collision model, TRIM [23], to obtain the recoil spectrum of 180keV Er ions on Pb. Using MD simulations as described elsewhere [3,4] we obtained the damage produced by 5keV Pb ions on Pb and 30 keV Pb ions on Pb. Figure 1 shows the results of one particular 5keV (figure 1a) and 30 keV (figure 1b) cascade in Pb. This figure shows the location of the vacancies (light circles) and the self-interstitials (dark circles) at the end of the collision cascade. Due to the low melting point of Pb, the melted area produced in the first few picoseconds of the collision cascade is very large therefore requiring of simulations containing at least one million atoms. Moreover, the total relaxation time for a cascade is also long: ~ 50 picoseconds (ps) for a 5keV cascade

and ~ 120 ps for 30 keV cascades, due to the low thermal conductivity of this material. These simulations were performed in a CRAY T3E, using 128 processors, with a CPU time of $\sim 10^{-6}$ s per time step and atom.. While the results from the MD simulations show the typical behavior of self-irradiated metals: vacancies are concentrated in the center of the cascade core with surrounding interstitials [2], these calculations clearly show the formation of dense interstitial and vacancy clusters after the cooling of the cascade. For the 30 keV case shown in figure 1b, 4 interstitial clusters were formed with an average number of 149 interstitial per cluster. 97% of all the interstitials produced are in the form of clusters.

The implantation of 180keV Er on Pb was simulated by KMC using the input data from MD described above. The implantation was carried out at -179°C to a total dose of 5×10^9 ions/cm². The thickness of the simulation box was 80nm, corresponding to the thickness of the TEM specimen in the experiments. Surfaces acted as perfect sinks for both vacancies and interstitials. After irradiation and before annealing free vacancies, vacancies in clusters and interstitials in clusters are present in the simulation. No single-interstitials or interstitial clusters of size smaller than 30 are present. Due to the low migration energy of these defects, and the one-dimensional motion, most of the interstitial clusters recombine with the surfaces even at this low temperature. Most of the vacancies form clusters, with just 27% of all vacancies as isolated defects.

The damage produced by the irradiation was annealed using a 10 minute per step temperature ramp: the temperature was increased by 50°C in 5 minutes and kept at a constant temperature for another 5 minutes. Figure 2 shows the results of the simulation for the total concentration of defects as a function of temperature. Initially most of the vacancies are in clusters (circles), there is a large number of interstitial in clusters (squares) and a few free vacancies (triangles). Between the implantation temperature and -140°C there is no change in defect concentration since all interstitials present are tied up in sessile clusters and vacancies are immobile. At temperatures above -140°C free vacancies start to move (arrow **a** in figure 2), corresponding to annealing stage III in Pb (between -123°C and -73°C) [24]. The number of free vacancies decreases while the number of vacancies in clusters increases. There is also at these temperatures a slight decrease in the interstitial cluster concentration due to recombination with free mobile vacancies. For temperatures higher than -80°C the concentration of vacancies in clusters decreases due to the dissolution of the smaller vacancy clusters (arrow **b** in figure 2), roughly corresponding to stage IV in Pb [24]. At the same time those vacancies recombine with the interstitial clusters, resulting in a reduction of the interstitial population. At temperatures between -80°C and 30°C the vacancy concentration decreases at a rate of 2.3×10^{15} Vacancies/cm³/°C. Notice that stage V, as obtained from resistivity measurements of electron irradiated Pb, occurs at a temperature of $\sim -3^{\circ}\text{C}$ and higher [24]. However, H. Schroeder and W. Schilling already pointed out that recovery processes for lower temperatures could be associated to the dissolution of smaller, less stable clusters, in good agreement with these simulations [24]. At these temperatures, the larger, more stable clusters do not dissolve. For temperatures between 30°C and 70°C the rate of disappearance of vacancies is 2.0×10^{16} Vacancies/cm³/°C, since at these temperatures even the larger clusters are dissolving. At a temperature of 70°C all

vacancy clusters have disappeared from the simulation box and only a few small interstitial clusters are present in the simulation.

The simulations showed that between -179°C and -63°C the cluster density increases by incorporating free vacancies that are mobile. The small clusters are stable at these temperatures and the vacancy cluster size distribution does not change significantly. Between -80°C and 20°C small vacancy clusters start dissociating, and the distribution shifts towards larger sizes, while the cluster concentration decreases, following Ostwald ripening. For temperatures larger than 20°C most of the vacancy clusters dissolve and there is a rapid decrease in defect density. Observe that by 63°C the cluster density is very small. At 70°C all clusters have disappeared. For the case of interstitials, the cluster size distribution moves towards smaller sizes with increasing temperature, since interstitial clusters do not break up at these temperatures, and disappear by dissolution through Vacancy-Interstitial recombination. The differences between distributions at -179°C and 20°C is small, since the number of free vacancies is small. At temperatures higher than 20°C, when large clusters of vacancies break up, the larger super-saturation of vacancies produces larger I-V recombination and the interstitial cluster sizes are greatly reduced, to end up with no interstitial clusters at a temperature of ~ 70°C.

In the validation experiments, which were carried out at LLNL, samples of high purity Pb were implanted with 180 keV Er ions at low doses ($\sim 5 \times 10^9$ ions/cm²) at a temperature of -183° C. The sample was cut in an edge in order to be later observed under the microscope. The sample was transported to the TEM and annealed *in situ*. The temperature was raised 50°C every 5 minutes and held for another 5 minutes before it was raised again. Figure 3 shows bright files images of the sample at different temperatures during the anneal: (a) as-implanted, (b) -116°C, (c) -60°C, (d) -5°C, (e) +13°C and (f) room temperature after anneal to 70 C. Loop densities were obtained from an area of $\sim 0.4 \text{ } \mu\text{m}^2$. The average diameter of the loops varied from a minimum of 4.7nm to a maximum of 9.1 nm at different temperatures during the anneal. It was found that as the temperature increases, so does the loop density. A maximum value is observed between -120°C and -10°C. At higher temperatures the loop density decreases and no loops are detectable under the microscope at temperatures of ~ 70°C.

In order to compare with the experimental results, we considered only those clusters containing more than 120 defects (interstitials or vacancies) corresponding to loops of radius $\sim 2\text{nm}$, assuming that the number of defects (N) in a loop is $N = 4 \text{ } R^2 / (3^{1/2} a_0)$. The density of vacancy clusters (open circles) increases with temperature with a peak at about 20°C, while the interstitial cluster density (squares) decreases for all temperatures. As a result there is a slight increase in the total population of loops up to a temperature of ~ 20°C. At higher temperatures the cluster density decreases and no clusters, either vacancies or interstitials, are present for temperatures higher than 70°C. This simulation shows good qualitative agreement with the experiments presented above. Better statistics both in the simulations and in the experiments are necessary in order to do a quantitative comparison of the results.

It is interesting to note that all visible interstitial clusters disappear in both the simulation and the experiments, even though the maximum anneal temperature is well below the melting point of Pb. One may expect that proximity of the free surfaces would mean that mobile vacancies would disappear before being able to recombine with interstitial clusters. However, because of the localized nature of defect production in cascades, the mobile vacancies dissolve the sessile interstitial clusters as they try to escape their nascent cascade and never escape to the matrix to become freely migrating defects.

In summary, these studies have shown that coupling experiments and simulations can lead to a detailed quantitative understanding of microstructure evolution in irradiated fcc metals such as Pb. The agreement between experiments and simulations gives us confidence that the model is indeed capable of describing the microscopic nature of damage production and evolution in irradiated metals. We demonstrated that production of defect clusters in the cascade core, followed by the subsequent mobility and clustering/dissolution kinetics of these clusters can explain the experimental observations. Further experiments and simulations are on the way in order to develop general, quantitative, and predictive models for radiation damage and defect evolution in metals.

III. Damage Production and Accumulation in Vanadium.

In the following, a brief example is given of a calculation that links MD and KMC simulations to extract the fraction of freely migrating defects in Vanadium [25]. Vanadium is the main constitutive element of a class of low activation materials that have been proposed for use in magnetic fusion reactors. These alloys exhibit good compatibility and radiation resistance, but questions remain regarding the helium embrittlement and the optimal temperature of operation that minimizes hardening and swelling.

We have carried out a set of MD calculations aimed at understanding defect production in Vanadium as a function of recoil energy. In addition, we have linked these MD results to KMC simulations of defect diffusion away from their nascent cascade in order to compute the temperature dependence of the fraction of freely migrating defects in this metal as well as the rate of damage accumulation in the presence of impurities. Figure 4 shows the primary damage state resulting from a 10 keV displacement cascade in vanadium at 300 K 15 ps after the recoil was launched. The crystal contained 500,000 atoms and the simulation was carried out on T3E parallel computer at NERSC. One key result of these simulations is the finding that very few defect clusters of either self interstitial or vacancy type are created at any recoil energy in Vanadium.

Next, we used the MD results, together with information on the energetics and kinetics of defects in Vanadium to compute the fraction of defects that are able to escape recombination within their nascent cascade as a function of recoil energy and temperature. This is the so-called fraction of freely migrating defects and its knowledge is key for the development of accurate mesoscopic theories of microstructure evolution under irradiation. Figure 5 shows a KMC calculation in a box 100nm on a side of the

escape ratio of (a) self interstitials and (b) vacancies as a function of recoil energy and temperature. The calculations were carried out for 100 s and thus serve to link the MD results at 10 ps to macroscopic time scales. The high mobility of the small interstitial clusters causes them to leave the box over the entire range of temperatures investigated, as seen in figure 6a. An interesting feature of this simulation is the correlation between recoil energy and escape ratio. The higher the recoil energy, the more defects produced, therefore the higher the probability for those defects to recombine and the lower the escape ratio. This observation is in contrast to similar work on other metals such as fcc Au and Cu in which the opposite or no dependence has been seen by us in other work. The type of lattice may play an important role in this difference. In fcc metals big dislocation loops are formed after the collision cascade and the vacancy rich core is clearly separated from the interstitials in the periphery.

The picture is considerably different for vacancies as shown in figure 5b. The low diffusivity of the single vacancy means its motion is not noticeable until temperatures of about 270 K, which is 100 degrees above the experimental temperature of stage III in this metal. At high recoil energies only the single vacancies have escaped after stage III has been reached, but small vacancy clusters still remain in the box. Only when the temperature is high enough for those clusters to break up and emit single vacancies can all the defects escape the box. This happens in stage V, which occurs at the second step located at 550K in the curves corresponding to the 5keV, 10keV and 20 keV recoils. The main conclusion of this study is that no production bias of vacancies occurs at any of the temperatures simulated. The fraction of FMD obtained for 20 keV recoils is 17% after normalizing by the NRT model.

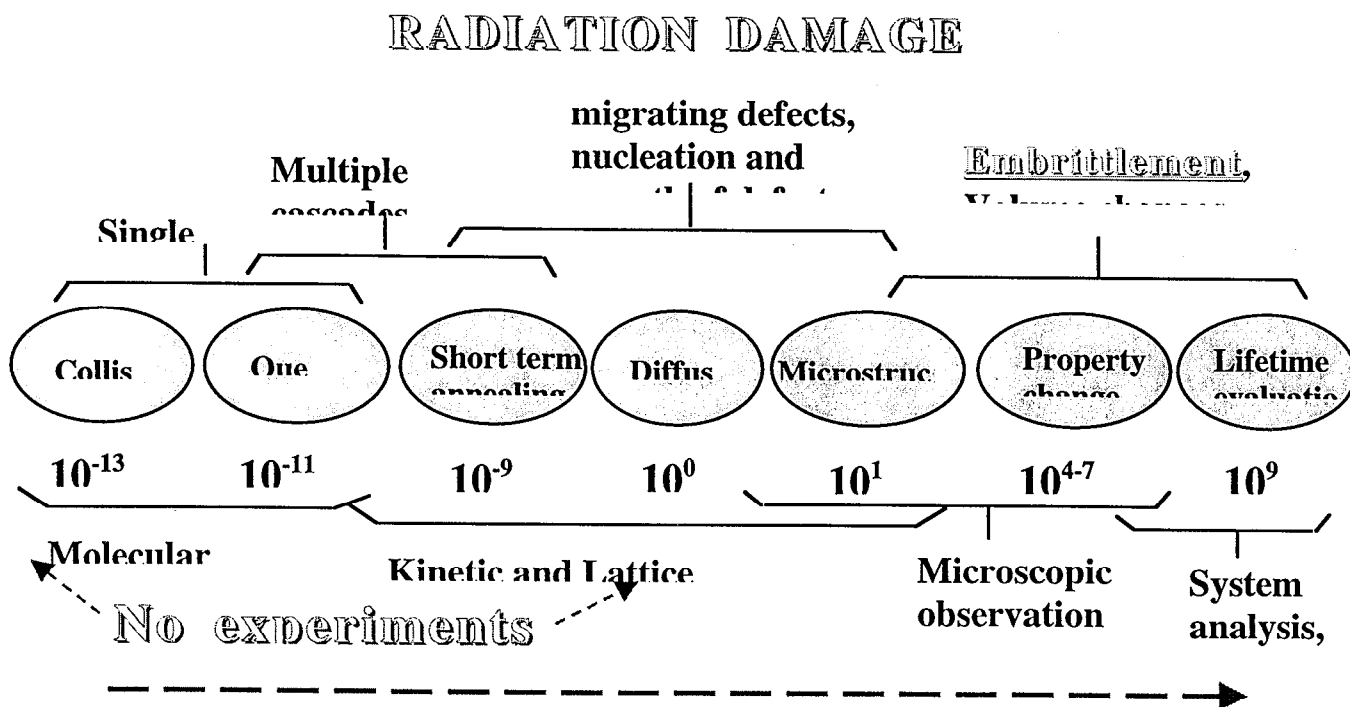
IV. Conclusions

In conclusion, we have shown how a hierarchy of simulation methods, based on the application of MD and KMC tools can serve to describe damage production, accumulation and annealing in irradiated metals. The simulations were compared to experiments where possible and the results showed that the methodology is not only useful, but can be quantitative and accurate for describing many problems in radiation effects.

The prospect of continued used and extrapolation of these methods rests on two key issues. On the one hand, one needs to obtain accurate interatomic potentials and defect data for different materials from first principles studies, and on the other there is a strong need for well defined, tailored experiments to validate the models along all stages of development. We argue that despite the difficulties ahead, the combination of ever increasing computer power and improving theoretical descriptions of materials properties will lead to improved and generally predictive models of radiation effects in a wide variety of materials.

This work is performed under the auspices of U.S. Department of Energy and Lawrence Livermore National Laboratory under contract No. W-7405-Eng-48.

FIGURE 1.



References

- [1] T. Diaz de la Rubia, Annual Review of Materials Science, **26**, (1996).
- [2] R.S. Averback, T. Diaz de la Rubia, In Spaepen and Ehrenreich (Eds) Solid State Physics, Vol. 51, Academic Press, New York, NY 1998, pp. 281-4021]
- [3] see e.g. *Fundamentals of Radiation Damage*, Ed. by I. Robertson, R.S. Averabck, D. Tappin and L.E. Rehn, J. Nucl. Mater.
- [4] R. Stoller, JOM **48**, 23 (1996).
- [5] D.J. Bacon, J. Nucl. Mater. **251**, 1 (1997).
- [6] D. J. Bacon and T. Diaz de la Rubia, *ibid.* Ref 3
- [7] K. Nordlund, M. Ghaly, R. S. Averback, et. al., Phys. Rev.B **57**, 7556 (1998)
- [8] R. Bullough, B.L. Eyre, and K. Krishan, Proc. Roy. Soc. **A346**, 81 (1975).
- [9] L. K. Mansur, in *Kinetics of Non Homogeneous Processes*, ed. G.R. Freeman (wiley, Ney York, 1987) p. 377
- [10] C.H. Woo and B.N. Singh, Philos. Mag. **A65**, 889 (1992).
- [11] B.N. Singh, S.I. Golubov, H. Trinkhaus, A. Serra, Yu. N. Osetsky, and A.V. Barashev, J. Nucl. Mater. **251**, 107 (1997).
- [12] W.G. Wolfer and M. Ashkin, J. Appl. Phys. **47**, 791 (1976).
- [13] A. Ryazanov, D. Braski, H. Schroeder, H. Trinkaus, J. Nucl. Mat. **233-237B**, 1076 (1996)
- [14] H. Huang, N. Ghoniem, J. Nucl. Mat. **250**, 192 (1997)
- [15] H. Heinisch, J. Nucl. Mater. **117**, 46 (1983).
- [16] H. Heinisch, B.N. Singh and T. Diaz de la Rubia, J. Nucl. Mater. **212-215**, 127 (1994).
- [17] H. Heinisch and B.N. Singh, J. Nucl. Mater. **191-194**, 125 (1992).
- [18] N. Soneda and T. Diaz de la Rubia, Philos. Mag. A, in press
- [19] T. Diaz de la Rubia, N. Soneda, M.J. Caturla and E.A Alonso, J. Nucl. Mater. **251**, 13 (1997).
- [20] G. R. Odette and B.D. Wirth, J. Nucl. Mater. **251**, 157 (1997).
- [21] H. Heinisch and B.N. Singh, J. Nucl. Mater. **251**, 77 (1997).
- [22] M. J. Caturla, E.A. Alonso, M. Wall, T. Diaz de la Rubia, and M. J. Fluss, Proceedings of the International Workshop on the Basic Aspects of the Differences in Radiation Damage between FCC and BCC metals and alloys. Cangas de Onis, Spain, October 1998. To be published in J. Nucl. Mater. 1999.
- [23] J. F. Ziegler, J. P. Biersack and U. Littmark in: Stopping and Range of Ions in Solids, vol. 1 (Pergamon, New York, 1985)
- [24] H. Schroeder, W. Schilling, Rad. Eff. **30**, (1976) 243
- [25] E.A. Alonso, M.J. Caturla, T. Diaz de la Rubia, and J.M. Perlado, Proceedings of the International Workshop on the Basic Aspects of the Differences in Radiation Damage between FCC and BCC metals and alloys. Cangas de Onis, Spain, October 1998. To be published in J. Nucl. Mater. 1999.

Figure 2a

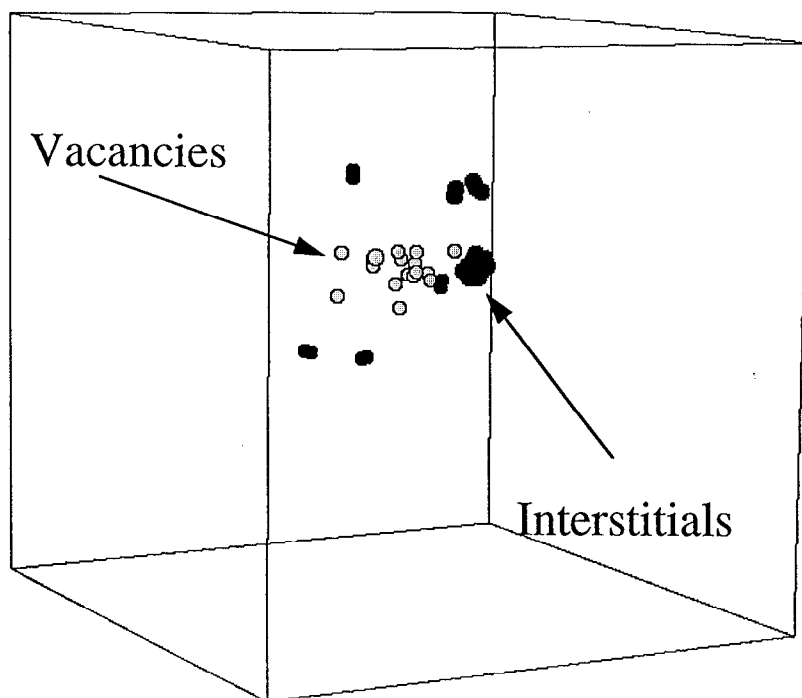


Figure 2b

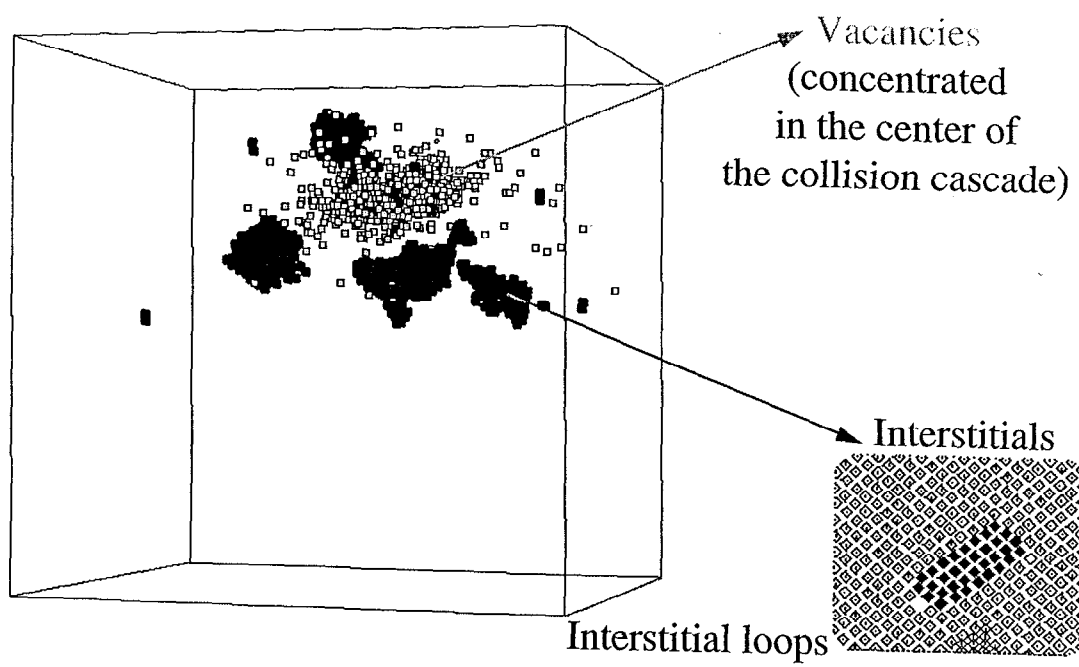


Figure 3

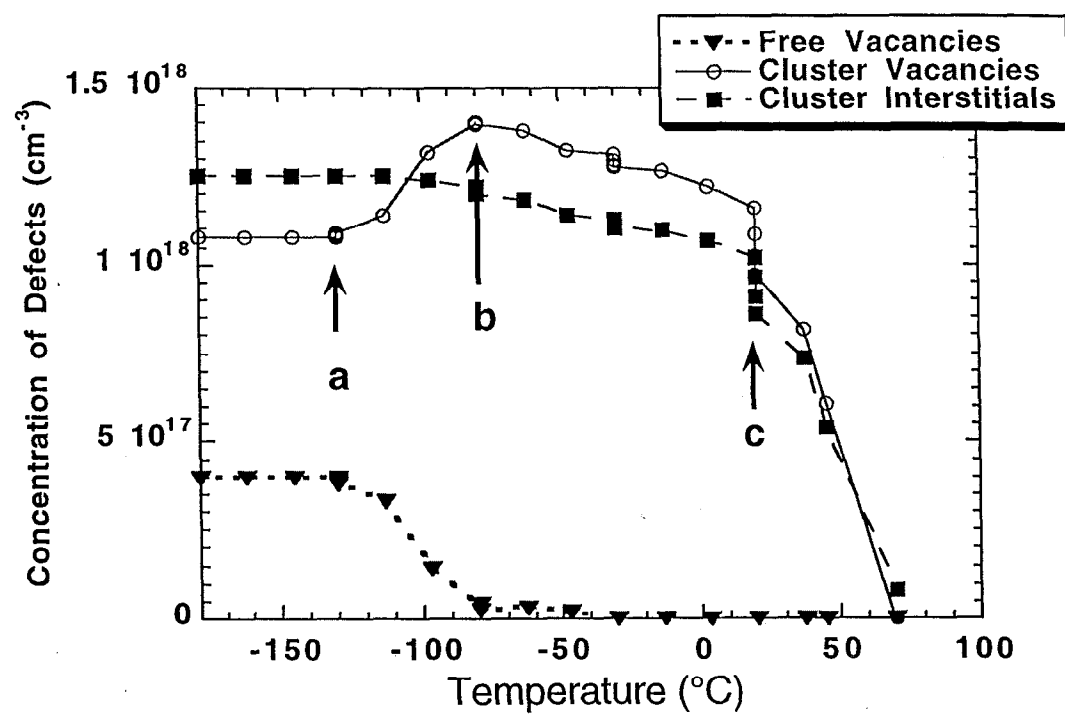
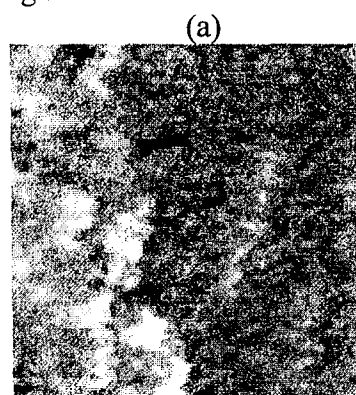
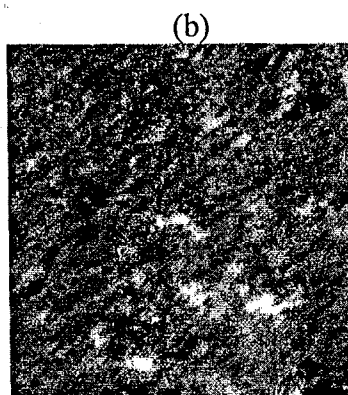


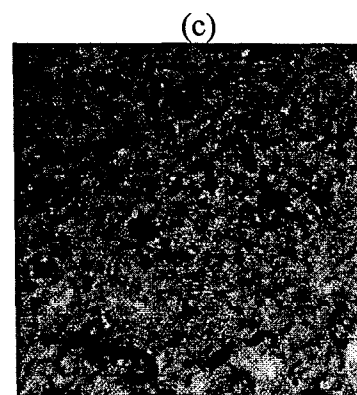
Figure 4



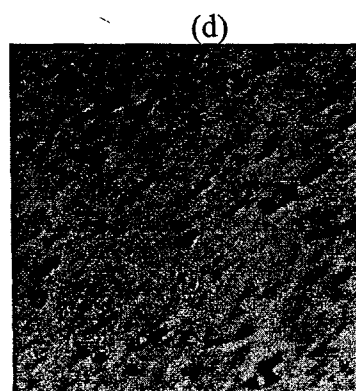
BF image @ -179 c, as implanted



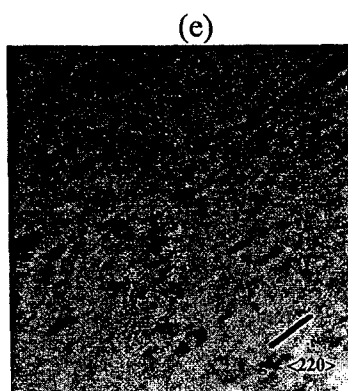
BF image @ -116 c



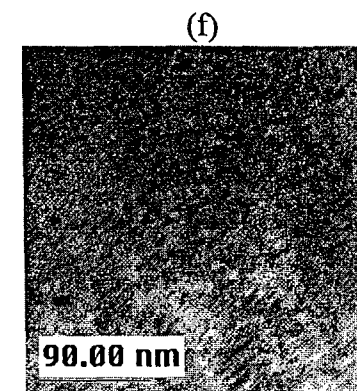
BF image @ -60 c



BF image @ -5 c



BF image @ +13 c



BF image @ room temp after
anneal to 70 c

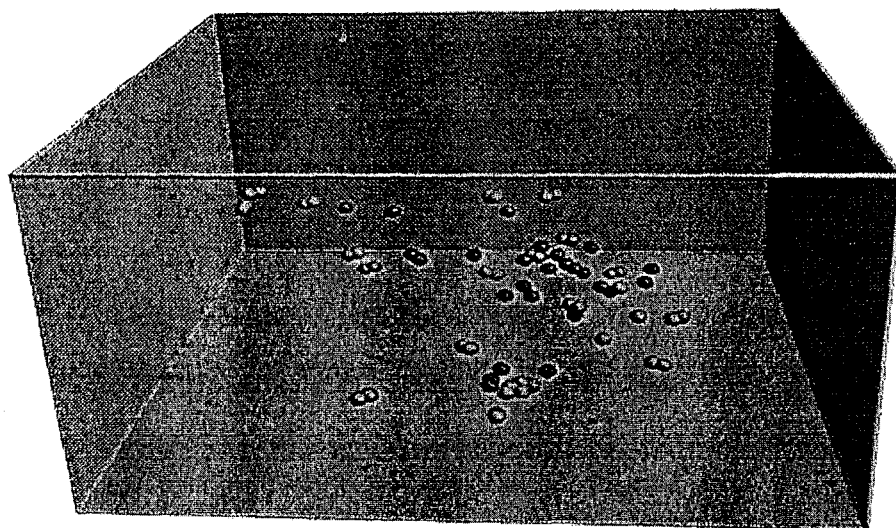


Figure 5. State of damage generated by a 10 keV PKA at 300K. The light points represent self-interstitial atoms and the dark ones vacancies. The defect population is stable 15 ps after the PKA entrance. No clusters larger than size 4 are formed.

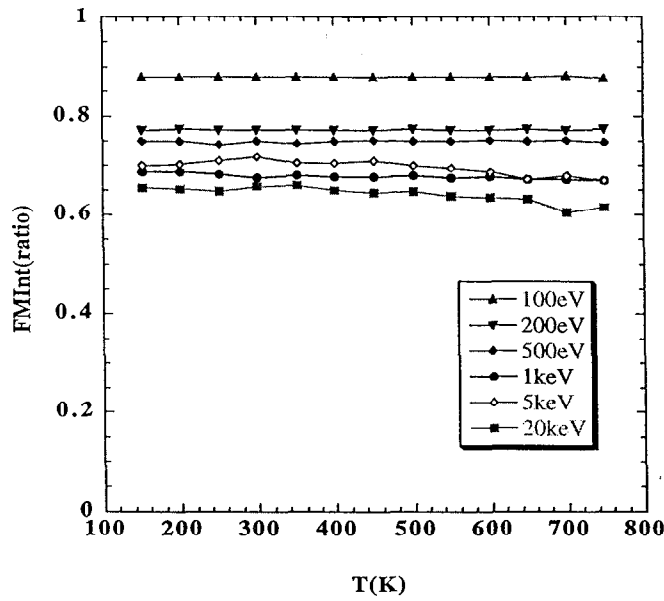


Figure 6a. Escape ratio of interstitials as a function of recoil energy and annealing temperature. Mobile interstitial clusters are also included in the escape ratio. Observe that the escape ratio decreases with increasing

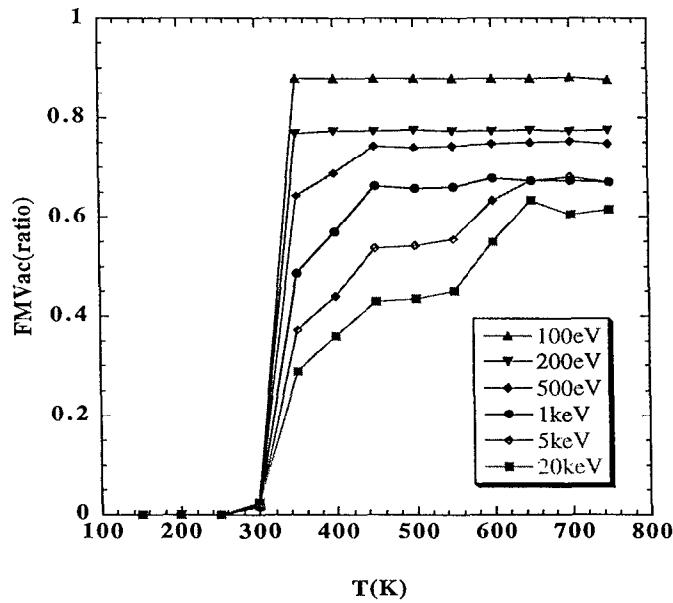


Figure 6b. Escape ratio of vacancies as a function of recoil energy and annealing temperature. The second step corresponding to stage V starts to be visible at PKA energies of more than 1 keV.